ADDITIVE MANUFACTURING OF MICRO FUNCTIONAL STRUCTURES THROUGH DIAMETER VARIABLE LASER STEREOLITHOGRAPHY AND PRECURSOR SINTERING HEAT TREATMENTS

Soshu Kirihara
Joining and Welding Research Institute, Osaka University
11-1 Mihogaoka Ibaraki 567-0047 Osaka, Japan

ABSTRACT

Stereolithographic additive manufacturing was customized successfully to create micro ceramics components. Photo sensitive acrylic resin with alumina of 170 nm in diameters was spread on a glass substrate with 5 to 10 μm in layer thickness by using a mechanical knife edge. Cross sectional layers patterned by ultraviolet laser scanning of 10 to 100 μm in variable diameter were laminated to create composite precursors. Dense components could be obtained through dewaxing and sintering heat treatments. Photonic crystals with periodic arrangements in magnetic permeability were created to control electromagnetic waves in terahertz frequency range by Bragg diffraction. The terahertz waves can synchronize with vibration modes of various biochemical molecules. Efficient terahertz wave resonators to excite the molecule vibrations will be specifically applied for novel analyzers and reactors. The photonic crystals including micro cavities were designed and fabricated successfully to resonate with microwaves in terahertz frequency range. The wave transmittances through the photonic crystals including the liquid cells were measured by using a terahertz time domain spectroscopy, and cross sectional profiles of electric field intensities were calculated by a transmission line modeling method.

INTRODUCTION

Periodic arrangements in dielectric constants can reflect electromagnetic waves through Bragg diffraction. Especially called photonic crystals theoretically exhibits forbidden gaps prohibiting wave transmissions[1]. The diffraction wavelengths are comparable to the lattice constants. Diamond type micro lattices with isotropic periodicities were processed as the perfect structure to open the photonic band gaps for all crystal directions[2]. However, special lattice propagations were difficult to create by conventional machining of molding processes. In our investigation group, ceramics photonic crystals with diamond structures were created by stereolithographic additive manufacturing and nanoparticles sintering. The band gap formation in the terahertz frequency ranges had been observed[3]. In this investigation, single and double cavities were introduced into the diamond photonic crystals in order to study the characteristic resonance modes by using computer aided design, manufacture and evaluation. These structural misfits can localize the electromagnetic waves strongly through multiple reflections, and wave amplification can realize transmission peak formations in the photonic band gaps according to the defect size[3].

Micro lattices with structural defects can be applied as wavelength filters in the terahertz frequency range. Terahertz waves with micrometer wavelengths and far infrared frequencies are expected to be used in various types of novel sensors to detect dust on electric circuits, defects on material surfaces, cancer cells in human skin, and bacteria in vegetables [4].

EXPERIMENTAL PROCEDURE

Diamond type photonic crystals with or without structural defects were designed using a graphics application (Magics 18, Materialise, Belgium) as shown in Fig. 1. Cavity defects of hollowed unit cells were arranged with center intervals of 1.5 and 2.0, as shown in Figs. 1 (a) and (b), respectively. Dielectric rods of coordination number 4 with an aspect ratio of 1.5 were connected with a coordination number of four to create a diamond structure with a 500 μm lattice constant. The designed model was converted into stereolithography files and sliced into a series of two dimensional layers. These numerical data were transferred to the stereolithographic equipment (SZ-1000S, Sezacc, Japan). Figure 2 shows a schematic illustration of the stereo- lithography fabrication process. Alumina particles (TM-DAR, Taimei Chemicals, Japan) of 170 nm in diameter were dispersed into a photosensitive acrylic resin at 40 vol. % by using a rotation and revolution mixing machine (SK-350T, Shashin Kagaku, Japan). The rotation and revolution speeds were 300 and 700 rpm, respectively. Fluid characteristics of the slurry paste were evaluated by a viscosity and viscoelasticity measuring instrument (VT550, Thermo Scientific, USA). Between two metal disks, the shear stresses were loaded by the rotating upper one on the lower one with a torque meter. The obtained slurry was squeezed onto the working stage from a dispenser nozzle and spread uniformly by a moving knife edge. The squeezing speed was 5 mm/s and the layer thickness was controlled to 10 μm. An ultraviolet laser of 355 nm in wave length is scanned on the ceramics slurry in order to create cross sectional planes with 5 μm in edge part accuracy. The laser beam was valued from 10 to 100 μm in spot size and from 10 to 200 mW in irradiation power. After the formation of the solid pattern, the elevator stage moved downward of 10 μm in the layer thickness, and then the next cross section is stacked. Three dimensional structures are fabricated by stacking all two dimensional layers. A microstructure was obtained through layer stacking of these cross sectional patterns. Uncured resin was removed by ultrasonic cleaning. The composite models were dewaxed at 600 °C for 2 hs and then sintered at 1500 °C for 2 hs in air. The heating rates were 1.0 and 8.0 °C/min in the dewaxing and sintering processes, respectively. The linear shrinkages of the created products were measured by digital optical microscopy (DOM) (VH-Z100, Keyence, Japan). The microstructures of the alumina lattices were observed by scanning electron microscopy (SEM) (JSM-6010LA, JEOL, Japan). A bulk sample of the sintered alumina was also fabricated to measure the relative densities by the Archimedes method. The transmission properties of the photonic crystals, with and without the structural defects, were analyzed to observe the band gap and the localized mode formation by using terahertz time-domain spectroscopy (THz-TDS) (J-Spec, Nippo Precision, Japan). The dielectric constant of the alumina lattice was measured in the

sintered bulk sample. A theoretical electromagnetic band diagram of the diamond photonic crystal was graphed through a plane wave expansion (PWE) application (Bandsolve, Rsoft, Japan). Intensity profiles of the structural defects in the presence of electric fields were simulated at localized mode frequencies using a transmission line modeling (TLM) simulator (Microstripes 7.0, Flomerics, UK).

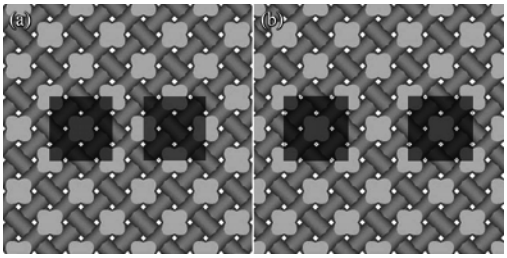

Fig. 1 Graphic models of diamond photonic crystals, with cubic defects indicated by dark areas. Unit cells were hollowed from the lattice structures in order to create double-cavity defects with 1.5 and 2.0 periods in center intervals, as shown in (a) and (b), respectively.

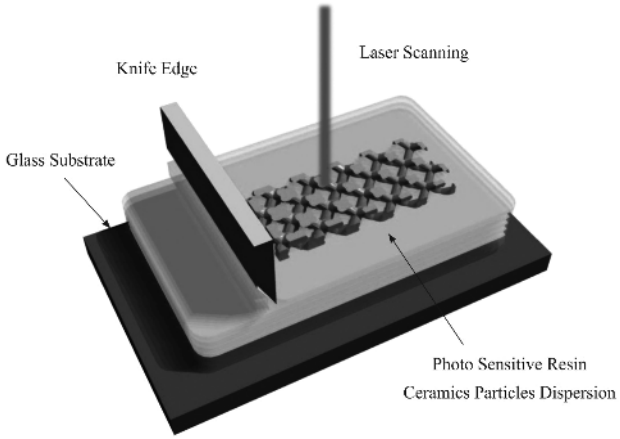

Fig. 2 A Schematic illustration of laser scanning stereolithography of additive manufacturing. Two dimensional layers solidified through laser scanning on photo sensitive resin including with nanoparticles are stacked up to create three dimensional components.

RESULTS AND DISCUSSION

An acryl photonic crystal including with alumina particles fabricated by the micro stereolithography is shown in Fig. 3-(a). The lattice constant of the formed diamond structure was 500 μm. The solid part tolerances can be measured as ±5 μm by DOM. The homogenized dispersions of the alumina particles in the acrylic resin matrix are observed by SEM as shown in Fig. 3-(b). Through the dewaxing and sintering processes, ceramic diamond structures were successfully obtained. Figure 4-(a) shows the sintered diamond structure composed of the micrometer order alumina lattice. The lattice constant and the linear shrinkage were measured by DOM. The lattice constant was measured as 375 μm. The deformation and cracking were not observed. The linear shrinkage on the horizontal axis was 23.8 % and that on the vertical axis was 24.6 %. It was possible to obtain the uniform shrinkage by designing an appropriate elongated structure in the vertical direction for compensation to the gravity effect. The alumina microstructure of 99 % in relative density is observed by SEM as shown in Fig. 4-(b). Dense alumina microstructure was formed, and the average grain size was approximately 2 μm. The forbidden band exhibited in the transmission spectra for the <111>, <100>, and <110> crystal directions were analyzed, and the dielectric constant of the alumina lattice was measured to be 9.0 by using THz-TDS. The higher and lower edges of the gap regions were plotted in the PWE calculated band diagram. The measured results were in good agreement with the calculated results, and a perfect photonic band gap was opened from 0.4 to 0.47 THz. The isotropic propagation of dense alumina lattices with a coordination number of four was verified. These results are evidence that the lattice structures had shrunk equally in all crystal directions without any dimensional deviations during the controlled dewaxing and sintering.

The diamond structure introduced by an air cubic defect with the same dimension as the unit cell is Fig. 5. The transmission spectrum along the Γ-X <100> direction is shown in Fig. 6. Two peaks were observed in the band gap at the frequencies 0.42 and 0.46 THz, respectively. Measured peak frequencies were compared with the simulation by the TLM method as seen in Fig. 7. They were in good agreement with the simulation. The first peak in Fig. 6 was named mode A, while the second one mode B. The electric field distributions of these modes were simulated by the TLM method. Fig. 8 (a) and (b) show cross sectional images of the distributions. In the images, the red area indicates that the electric field intensity is high, whereas blue and green area indicates it is low. Thus, it was considered that the mode A concentrated the oscillation energy of a half wavelength with an antinode in the cube. Also, the mode B concentrated the energy of a half wavelength on the sides of the cube with a node in the cube. Therefore, it was confirmed that the defect introduced structure localized terahertz waves.

The double cavity defects were introduced into the alumina photonic crystals by hollowing the unit cells of the diamond lattices, as shown in Fig. 9. The intensity profiles of electric fields in the vicinity of double cavity defects arranged with 1.5 and 2.0 periods in center intervals, respectively, were simulated by TLM as show in Figs. 10 (a) and (b). The electro-

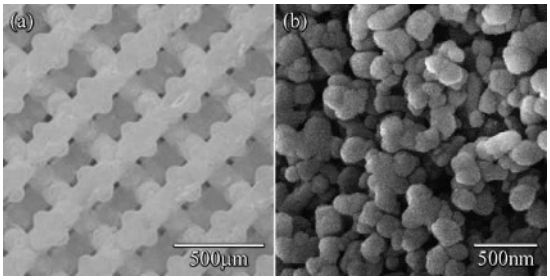

Fig. 3 Precursor of the photonic crystal fabricated by stereolithography: (a) Acryl rods with a coordination number of 4 and (b) homogenized dispersion of alumina nanoparticles.

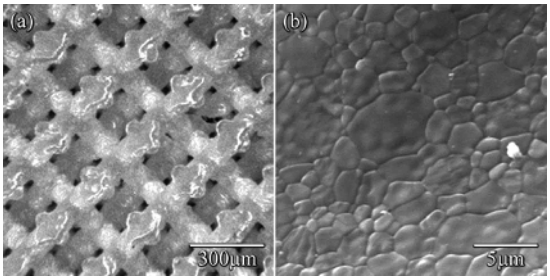

Fig. 4 Full ceramic component of the photonic crystal processed through the dewaxing and sintering. (a) Alumina microlattices with (b) fine microstructure were formed successfully.

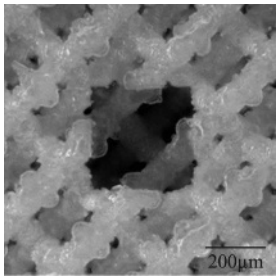

Fig. 5 An alumina lattice with the diamond structure, into which a cubic air defect has been introduced. The edge length of the air cavity is the same size as the lattice constant.

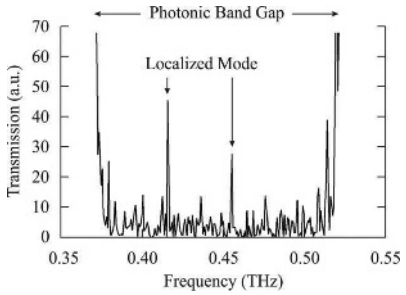

Fig. 6 Transmission spectrum of a structure into which a defect has been introduced. Two peaks representing localized modes of transmission occur in the photonic band gap.

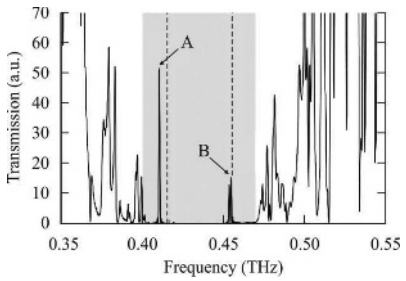

Fig. 7 Simulated spectrum of the structure with the defect. The dashed lines indicate the measured peaks. The frequency range with gray shading indicates the perfect band gap.

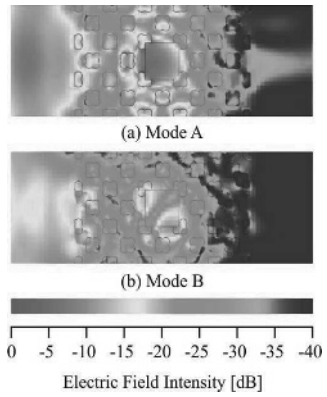

Fig. 8 Electric field distributions of localized mode A (a) and mode B (b) simulated by TLM, using the finite difference time domain (FDTD) technique.

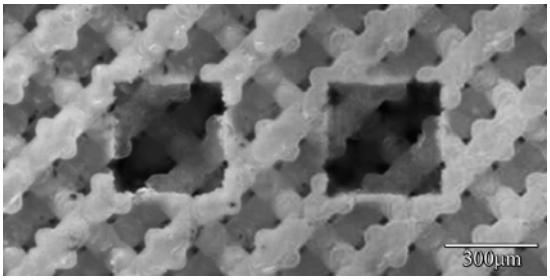

Fig. 9 Sintered alumina lattices with double-defect cavities. The unit cells were hollowed from the diamond structure. The cubic cavities were separated by one period of the lattice .

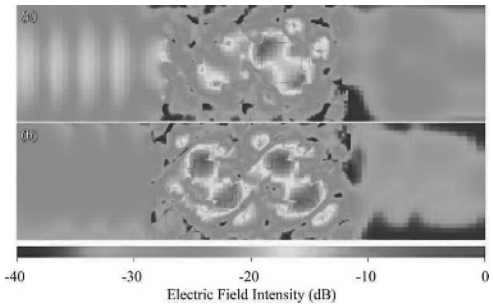

Fig. 10 Intensity profiles of electric fields in the defect cavities. The localized modes were formed in the cavities arranged with 1.5 (a) and 2.0 (b) periods in center intervals.

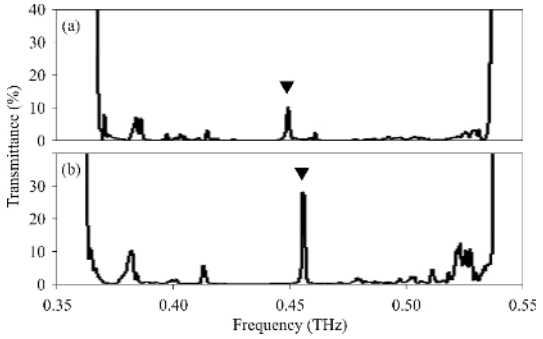

Fig. 11 Transmission amplitude of the terahertz waves through the photonic crystal with defect cavities. The transmission peaks, indicated the solid triangles, were formed thorough localization into the double cavities separated by the 1.5 and 2.0 period, as shown in (a) and (b), respectively.

magnetic waves resonated and localized in the cubic cavities. The single resonance mode spread in the vicinity of closed cavities, and the coupled mode was localized strongly in the separated dual cavity. The transmission spectra, including the photonic band gaps and localized modes, were analyzed by the THz-TDS. As shown in Figs. 11 (a) and (b), the localized mode peaks with transmission intensities of 5 and 27 % formed at 0.45 and 0.56 THz, respectively, through the double-cavity defects separated by the 1.5 and 2.0 periods. The spread mode formed a small resonance peak at the longer wavelength of the lower frequency. The concentrated mode realized sharp and clear peak formation with the higher transmission intensity.

CONCLUSIONS

Through stereolithographic additive manufacturing and nanoparticles sintering, alumina photonic crystals with diamond structures were successfully fabricated in order to control terahertz waves through Bragg diffraction. Acryl models with alumina nanoparticles were dewaxed and sintered carefully and fine diffraction lattices were obtained according to the designed models. By the introduction of single and double cavities could, localized modes of transmission peaks could be created in complete band gaps. Filtering properties at specific wavelengths can be applied in sensor devices.

REFERENCES

[1]K. Ohtaka, Energy Band of Photons and Low-energy Photon Diffraction, Physical Review B, 19 [10] (1979) 5057-5067.

[2]K. M. Ho, C. T. Chan and C. M. Soukoulis, Existence of a Photonic Gap in Periodic Dielectric Structures, Physical Review Letters, 65 [25] (1990) 3152-3155.

[3]S. Kirihara, Y. Miyamoto, International Journal of Applied Ceramic Technology, 6 (2009) 41.

[4]B. Temelkuran, Mehmet Bayindir, E. Ozbay, R. Biswas, M. M. Sigalas, G. Tuttle and K. M. Ho, Photonic crystal-based Resonant Antenna with a Very High Directivity, Journal of Applied Physics, 87 [1] (2000), 603-605.

[5]H. Yada, M. Nagai, and K. Tanaka, The Intermo-lecular Stretching Vibration Mode in Water Isotopes Investigated with Broadband Terahertz Time-domain Spectroscopy, Chemical Physics Letters, 473 [4-6] (2009) 279–283.